Galerkin-type coupled Boundary Element Method for Time domain simulations on Discontinuous surfaces

Moritz Hartmann[a], Nicolas Desmars[a], Marco Klein[a], Norbert Hoffmann[b,c] , Jasper Behrendt[c], Jakob Schwarz[b,c]
a. Institute of Maritime Energy Systems, German Aerospace Center, 21502 Geesthacht
b. Dynamics Group, Hamburg University of Technology, 21073 Hamburg
c. BHS Hamburg, 22761 Hamburg
Email: moritz.hartmann@dlr.de

Highlights

Galerkin BEM, High-order spectral method, Discontinuous domains, Hydrodynamics

1 Introduction

Boundary element methods (BEMs) are widely used in the field of marine hydrodynamics for the analysis of wave-ship interaction. Even if a large variety of BEM solvers exists (e.g. based on the free surface Green function method, on the Rankine-source Green function approach or on boundary integral equation solvers), most approaches do not consider the free surface discontinuity due to the presence of the body in the near-field assembly of boundary integral operators (BIOs). In consequence, complex computational grids, which need to be updated for nonlinear time domain simulations, are required.
In the context of this abstract, we present the 2D and linearized Galerkin-type coupled BEM (cBEM) that solves for the mixed boundary value problem (BVP) containing the discontinuous free surface and body surface, c.f. Fig. (1). The incorporation of the high-order spectral (HOS) method, introduced by West et al. (1987) and Dommermuth & Yue (1987), allows the monolithic coupling of wave and body dynamics. In the presented application, small amplitude motions of a surface piercing body around its equilibrium position are considered. High-order basis functions are used to approximate the solution function space composed of the velocity potential ϕ and its normal derivative $\partial\phi/\partial\mathbf{n}$, and the geometry of the body. We discuss the verification of cBEM with an analytic reference solution and demonstrate the validity of the solver for hydrodynamic problems with experimental and numerical data.

2 Mathematical foundation

The considered mixed BVP was given by

$$\Delta\phi(\mathbf{x}) = 0 \qquad \text{for } \mathbf{x} \in \Omega \tag{1.1}$$

$$g_D(\mathbf{x}) := \phi(\mathbf{x}, t) \qquad \text{for } \mathbf{x} \in \Gamma_{W,D} \tag{1.2}$$

$$g_N(\mathbf{x}) := \frac{\partial\phi(\mathbf{x}, t)}{\partial\mathbf{n}} \qquad \text{for } \mathbf{x} \in \Gamma_{B,N} \tag{1.3}$$

$$\phi = 0, \quad \frac{\partial\phi}{\partial\mathbf{n}} = 0 \qquad \text{for } |r| \to \infty\ , \tag{1.4}$$

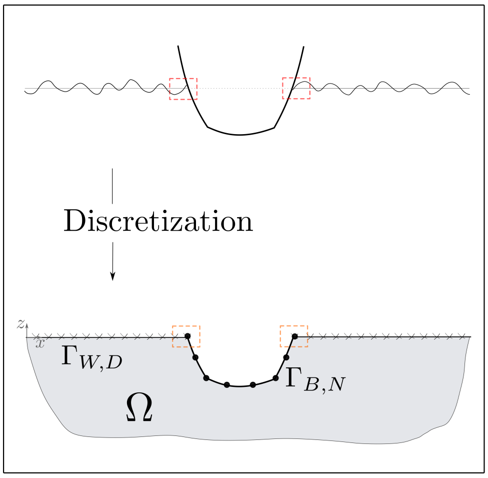

(a) Problem of interest and discretization.

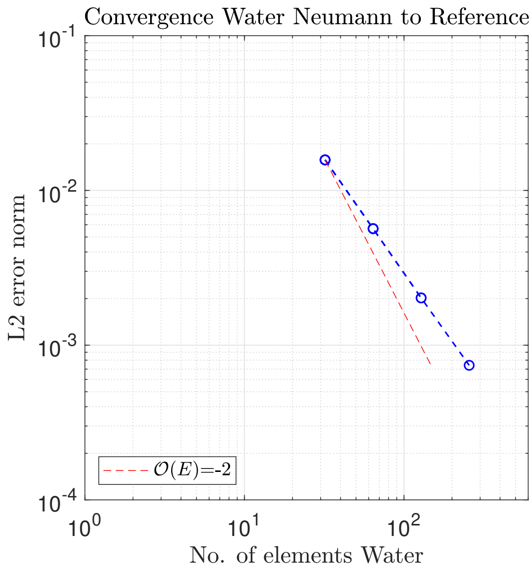

(b) Convergence of cBEM solution (bullets).

Figure 1: (a) Mixed BVP with surface discontinuities and (b) L_2-error of cBEM result against the analytic reference for the stationary, surface piercing body test case. The red colored dashed line in (b) represents the slope equivalent to convergence order $|\mathcal{O}(E)| = 2$.

with $\mathbf{x} = (x, z)$. The Laplace equation, Eq. (1.1), together with the Dirichlet problem, Eq. (1.2), at the free surface and the Neumann problem, Eq. (1.3), at the body surface, was written in terms of the Boundary Integral Equations (BIEs) in the Galerkin formulation

$$\begin{aligned}\int \psi(x)\gamma_0^{ext}\phi(x)\mathrm{d}s_x = \int \psi(x)\Big[\int G(x,y)\frac{\partial\phi(y)}{\partial\mathbf{n}(y)}\mathrm{d}s_{y,W} - \int \frac{\partial G(x,y)}{\partial\mathbf{n}(y)}\phi(y)\mathrm{d}s_{y,W} + \\ \int G(x,y)\frac{\partial\phi(y)}{\partial\mathbf{n}(y)}\mathrm{d}s_{y,B} - \int \frac{\partial G(x,y)}{\partial\mathbf{n}(y)}\phi(y)\mathrm{d}s_{y,B}\Big]\mathrm{d}s_x = 0\end{aligned} \tag{2}$$

$$\int \psi(x)\gamma_1^{ext}\phi(x)\mathrm{d}s_x = \int \psi(x)\big[\mathbf{n}(x)\cdot\nabla(x)\gamma_0^{ext}\phi(x)\big]\mathrm{d}s_x = 0 \tag{3}$$

with $G(x,y) = -\frac{1}{2\pi}\log(|x-y|)$, denoting the 2D Green function that represents the fundamental solution to the 2D Laplace equation, and the test-function ψ. The exterior trace operator and its normal derivative, γ_0^{ext} and γ_1^{ext}, represent the limiting-to-the-boundary process, which enables access to boundary values. In addition to the conditions proposed in Eq. (1), the Method of Farfield Extension was used on the free surface domain to approximate periodicity in the lateral dimension. Combining the conventional BIE, Eq. (2), and the normal derivative BIE, Eq. (3), and reordering, gave the direct formulation in block matrix form

$$\begin{pmatrix}\mathcal{A}+\sigma & \mathcal{H}\\ \mathcal{S} & -\mathcal{D}+\sigma\end{pmatrix}\begin{pmatrix}\frac{\partial\phi}{\partial\mathbf{n}}\\ \phi\end{pmatrix} = \begin{pmatrix}\mathcal{H} & \mathcal{A}\\ -\mathcal{D} & \mathcal{S}\end{pmatrix}\begin{pmatrix}g_D\\ g_N\end{pmatrix} \tag{4}$$

including the free term σ and the Single-layer ($\mathcal{S}$), Double-layer ($\mathcal{D}$), Adjoint ($\mathcal{A}$), and Hypersingular ($\mathcal{H}$) BIOs defined by

$$\begin{aligned}\mathcal{S}\frac{\partial\phi}{\partial\mathbf{n}_y} &= \int\psi(x)\int G\frac{\partial\phi}{\partial\mathbf{n}_y}(y)\mathrm{d}s_y\mathrm{d}s_x, \quad \mathcal{D}\phi = \int\psi(x)\int\frac{\partial G}{\partial\mathbf{n}_y}\phi(y)\mathrm{d}s_y\mathrm{d}s_x,\\ \mathcal{A}\frac{\partial\phi}{\partial\mathbf{n}_y} &= \int\psi(x)\int\frac{\partial G}{\partial\mathbf{n}_x}\frac{\partial\phi}{\partial\mathbf{n}_y}(y)\mathrm{d}s_y\mathrm{d}s_x, \quad \mathcal{H}\phi = \int\psi(x)\int\frac{\partial^2 G}{\partial\mathbf{n}_x\partial\mathbf{n}_y}\phi(y)\mathrm{d}s_y\mathrm{d}s_x,\end{aligned} \tag{5}$$

with $\mathbf{n}_x = \mathbf{n}(x)$, $\mathbf{n}_y = \mathbf{n}(y)$ and $G = G(x, y)$. The weighting of the BIEs, Eqs. (2) and (3), with the test-function in the context of the Galerkin approach, made the integration over both field- and test-function domain in the operator assembly necessary and the (hyper)singular integral kernels were evaluated by means of the direct desingularization approach introduced by Bonnet & Guiggiani (2003). The approximation of the solution for the free surface was done using Z-Spline basis functions, see Sagredo (2003), that allowed to replace the global basis functions of the HOS method by basis functions of compact support. Consequently, the free surface discontinuity due to the surface piercing body could be treated explicitly by using new integration limits at the intersection elements. In Fig. (1.a), the intersection elements are highlighted by the colored dashed boxes. Besides the Z-Splines, basis function of interelement-type (support beyond one element) and intraelement-type (support restricted to one element) B-Splines for the solution approximation at the body surface were used. The linear wave equations were integrated in time by using the fourth-order Runge-Kutta scheme.

3 Numerical results and discussion

The verification and validation of cBEM are summarized in the next paragraphs.

Verification cBEM We verified cBEM by considering the analytic solution of the velocity potential in deep water provided by the 2D Linear Wave Theory

$$\phi_{lin}(x, z; t) = -i\frac{\hat{\eta}g}{\omega}\mathrm{e}^{i(kx-\omega t)}\mathrm{e}^{kz} \qquad (6)$$

wherein the amplitude of the surface elevation is denoted by $\hat{\eta}$, the gravitational acceleration by g, the wavenumber is k, related to the wave angular frequency ω through the linear deep water dispersion relation. Based on Eq. (6), the Dirichlet and Neumann reference data at the water surface and the body surface were derived and inserted in the linear block matrix system Eq. (4). After solving it, the results were compared with the numerical results of cBEM. Figure (1.b) shows the error after one solution evaluation between the analytic reference and the cBEM results by means of the weighted L_2-norm for the surface piercing body with radius $r_B = 4\,\mathrm{m}$, centered in the free surface domain of length $L_W = 32\,\mathrm{m}$. The convergence of the solution of $\partial\phi/\partial\mathbf{n}$ with increasing number of water elements is of order $|\mathcal{O}(E)| = 1.47$. The low error in the range of 10^{-3} verified the self- and near-field assembly methods, as well as the procedure for evaluating the coupling operators representing the influence of the water to the body boundary domain and vice versa.

Application to hydrodynamics To validate cBEM, the radiation of waves due to forced and oscillating, small amplitude heave motions of a surface piercing rectangular cylinder was analyzed in terms of the added mass and the damping coefficient. In Fig. (2), we compare the time domain results of cBEM after reaching a converged state with the experimental and computational reference data given in Vugts (1968) over the investigated oscillation frequency range. It is shown that the numerical results of cBEM are well comparable to the reference data over the complete parameter range for both the damping coefficient (blue) and the added mass (red).

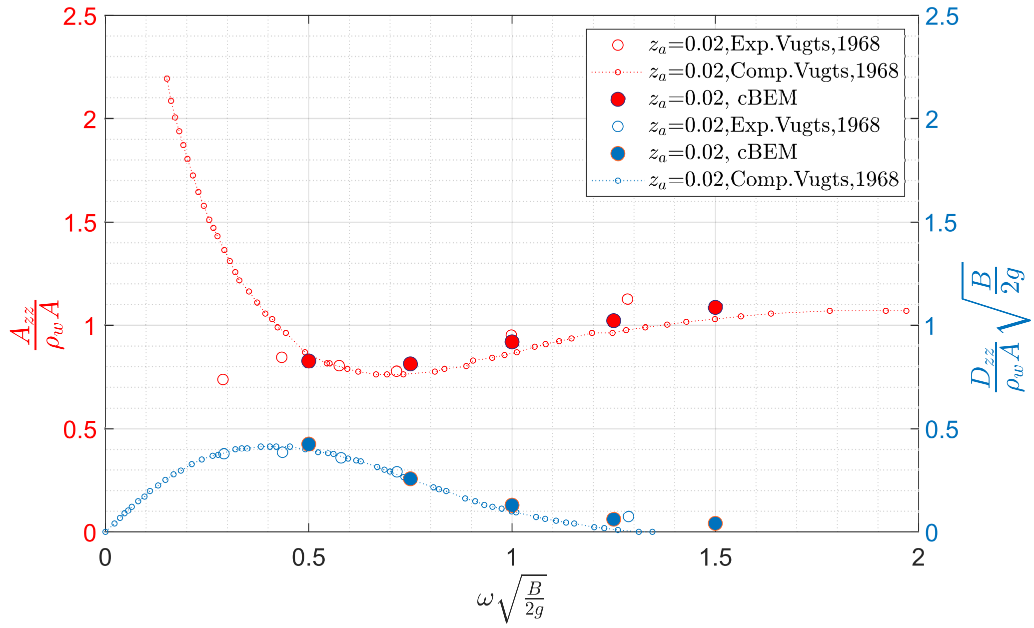

Figure 2: Normalized added mass (red) and damping (blue) coefficient for the surface piercing cylinder at different oscillation frequencies compared to results of Vugts (1968).

4 Conclusion

The solver cBEM was investigated with an analytic reference and literature data for the case of a free surface piercing body in regular linear waves. The development of desingularization methods for the coupling operators allowed the explicit consideration of the discontinuous free surface and body surface. The use of a regular grid, which does not have to be adapted to the body surface nor updated at each time step, gives a time-saving alternative to classical BEM approaches. Future steps are the consideration of intersections between the elements, the incorporation of the body dynamics, the extension to nonlinear wave dynamics and the implementation in 3D.

References

Bonnet, M. & Guiggiani, M. (2003), 'Direct evaluation of double singular integrals and new free terms in 2d (symmetric) galerkin bem', *Computer methods in applied mechanics and engineering* **192**(22-24), 2565–2596.

Dommermuth, D. G. & Yue, D. K. (1987), 'A high-order spectral method for the study of nonlinear gravity waves', *Journal of Fluid Mechanics* **184**, 267–288.

Sagredo, J. T. B. (2003), Z-splines: moment conserving cardinal spline interpolation of compact support for arbitrarily spaced data, *in* 'Research Report/Seminar für Angewandte Mathematik', Vol. 2003, ETH, Eidgenössische Technische Hochschule Zürich.

Vugts, J. H. (1968), 'The hydrodynamic coefficients for swaying, heaving and rolling cylinders in a free surface', *International Shipbuilding Progress* **15**(167), 251–276.

West, B., Brueckner, K., Janda, R., Milder, D. & Milton, R. (1987), 'A new numerical method for surface hydrodynamcis', *Journal of Geophysical Research* .